Gulf Stream rings as a source of iron to the North Atlantic subtropical gyre

Journal Article

Author(s):
Conway, Tim M.; Palter, Jaime B.; De Souza, Gregory

Publication date:
2018-08

Permanent link:
https://doi.org/10.3929/ethz-b-000275780

Originally published in:
Nature Geoscience 11(8), https://doi.org/10.1038/s41561-018-0162-0

Funding acknowledgement:
708407 - Southern Ocean Silicon Cycling: combining views of the past and present using silicon isotopes (EC)

Gulf Stream rings as a source of iron to the North Atlantic subtropical gyre

Tim M. Conway[1,2,*,#], Jaime B. Palter[3,#] and Gregory F. de Souza[2,#]

[1] College of Marine Science and School of Geosciences, University of South Florida, St Petersburg, FL, USA
[2] Institute of Geochemistry and Petrology, ETH Zürich, Department of Earth Sciences, Zürich, Switzerland
[3] School of Oceanography, University of Rhode Island, RI, USA.

*Corresponding author: *tmconway@usf.edu*; Phone: +1 727 553 3408
[#] All authors contributed equally to this work.

Keywords: GEOTRACES, biogeochemistry, nutrient supply, micronutrients, mesoscale

Substantial amounts of nitrogen fixation occur in the North Atlantic subtropical gyre[1], due to the activities of cyanobacteria with high iron requirements[2]. Iron is delivered to this region by dust from the Sahara[3]. However, this dust deposition is typically localised and episodic. Therefore, other sources of iron may also be important. Here, we report observations of dissolved iron concentrations in a Gulf Stream cold-core ring, which transported iron-rich water from near the continental slope into the subtropical gyre. We find that iron concentrations were elevated in the ring compared to subtropical waters, reflecting its source waters. Using iron data from these source waters and the identification of ring activity in satellite data, we estimate that cold-core rings provide a net flux of 0.3±0.17×10^{8} mol Fe yr^{-1} across the north-western gyre edge, on the order of 15% of our median estimates of gyre-wide supply of iron by dust deposition. We suggest that iron supply from cold core rings is an important source of iron to the northwestern gyre edge. We conclude that mesoscale ocean circulation features may play an important role in subtropical nutrient and carbon cycling.

Iron sources to the North Atlantic subtropical gyre. Primary productivity in much of the Southern Ocean as well as the equatorial and sub-Arctic Pacific has been shown to be limited by iron (Fe)[4,5]. In contrast, in oligotrophic regions of the ocean such as the North Atlantic subtropical gyre (NASG), productivity is thought to be limited instead by macronutrients, and thus much less sensitive to Fe addition[5,6]. Owing to its proximity to the Sahara Desert, the North Atlantic receives the largest atmospheric dust fluxes globally[3], resulting in dissolved Fe concentrations of up to 2 nmol kg^{-1} in surface waters[5]. It has therefore long been assumed that dust provides ample Fe for phytoplankton to utilise available macronutrients in this region. However, the degree to which Fe from dust dissolves in seawater and is stabilised therein by organic ligands is widely debated[7]. Moreover, dust deposition is highly localised and episodic, varying dramatically with storm activity, location and season[3,8,9], and may quickly overwhelm the capacity of seawater and organic ligands to maintain the supplied Fe in solution, leading to increased precipitation and scavenging losses. In fact, dissolved Fe concentrations at the surface in the western gyre can be as low as 0.09 nmol kg^{-1} during winter, with a potentially growth-limiting dissolved Fe minimum (0.02-0.20 nmol kg^{-1}) present in subsurface waters (50-150 m) year-round[9,10]. Background Fe concentrations of the gyre in the absence of dust deposition are also reproducibly low (Suppl. Info.). In addition to limiting nitrogen uptake in the North Atlantic[11], a recent study has found that Fe may also limit phosphate acquisition by the microbial community in the North Atlantic in areas distal from the Saharan dust plume[12]. Therefore, all sources of Fe must be considered for their potential to fuel primary productivity within the gyre.

Gulf Stream rings. As early as the 1930s, scientists discovered boluses of anomalously cold water in the NASG and inferred that eddies must transport water from the Slope Sea, which lies between the continental shelf and the Gulf Stream, into the gyre[13]. These 'cold-core rings' are formed when a Gulf Stream meander becomes so large that it folds back onto itself, forming a loop that pinches off from the main current. These rings trap Slope Sea water, and are easily identifiable in satellite observations as they propagate into the subtropical gyre, characterised by a circular depression of sea-surface height. Although it has been proposed that eddy-driven, cross-Gulf Stream transport constitutes an important supply of phosphorus (P) to the subtropical gyre[14], and it is well known that lateral processes in general play a role in supplying macronutrients to the gyres[15–18], the effect of Gulf Stream rings on Fe transport has not been considered, largely due to a paucity of high-quality Fe data. Here, by combining a recent satellite-derived dataset of mesoscale eddy activity[19] with a new dissolved Fe dataset[10] from a North Atlantic GEOTRACES section[20,21] (GA03; Fig. 1), we quantify the potential of Gulf Stream rings to supply Fe to the NASG. The GA03 dataset is the first able to provide this insight, with two stations located in the Slope Sea, several within the NASG, and one station (USGT11-6) serendipitously situated at the edge of a Gulf Stream cold-core ring (Fig. 1).

Cross Gulf Stream iron transport. Slope Water is identifiable in the GA03 section by its low temperature and salinity (Figs 2-3), and is characterised by high concentrations of macronutrients[21] and CFCs[20], reflecting upwelling of nutrient-rich water and contributions from shelf and Labrador Sea Water sources[21,22]. Slope Water is also greatly enriched in dissolved Fe compared to waters of equivalent density in the subtropical gyre[10] (Fig. 3; 0.64 vs. 0.30 nmol kg^{-1} above the 1026.5 isopycnal; Methods). These higher Fe concentrations have been attributed to a margin sediment source, which is important throughout the mid-depth (~600-2000 m) subtropical North Atlantic[10]. Within the subtropical gyre, however, a wedge of Fe-depleted Subtropical Mode Water (STMW)[23] separates this enriched mid-depth layer from the surface (Fig. 2). The cold-core ring sampled along GA03 transports Slope Sea water into the Fe-depleted gyre, with dissolved Fe concentrations 25% higher above the 1026.5 isopycnal, and 60% higher above 500 m, than the open gyre (Figs 2-3).

The observation of a ring of Fe-rich Slope Water within the Fe-poor subtropical gyre suggests that rings could represent a significant source of Fe to the NASG, assuming the GA03 observations of the difference between gyre and Slope Sea Fe concentrations are characteristic for the region. Such as assumption is justified for a number of reasons, as discussed here and in more detail in the Supplementary Information. Firstly, the Fe-poor nature of the NASG waters is well documented; not only do the US GEOTRACES GA03 zonal section[10] (2011) and the separate Dutch GEOTRACES GA02 meridional transect[24] (2010) both show consistently low Fe concentrations through waters of the subtropical gyre, but three station reoccupations near Bermuda also provide evidence for the temporal stability of low Fe concentrations in the NASG over a period of three years[25,26]. The temporal variability of Slope Sea Fe concentration cannot be similarly directly assessed since the Fe concentration of its subsurface waters has not been previously reported. However, the propagation of characteristic sediment-derived Fe stable isotope compositions into the ocean interior[10] suggests that the Slope Sea Fe is relatively long-lived, consistent with the observation here of elevated Fe within a ring that was shed 5-6 weeks before sampling (Fig. 2; Suppl. Anim. 2; Methods). Furthermore, earlier work describes a qualitatively similar gradient of high Fe in very surface North American shelf waters decreasing into the open gyre[27]. At the basin scale, water column Fe datasets from reoccupied ocean stations in three other regions of the ocean, both with and without proximal sediment sources, also indicate the relative temporal stability of Fe profiles, similar to the macronutrients, at least on a sub-decadal timescale[20,26,28]. We thus feel confident in using the GA03 Fe data as sufficiently representative of the system in order to calculate the contribution of ring-driven transport to the Fe budget of the gyre.

This ring-driven Fe transport flux depends on: 1) the number of rings that cross the Gulf Stream per year, 2) the amount of dissolved Fe each ring carries, and 3) the fraction of this transported Fe that remains within the gyre rather than being re-entrained into the Gulf Stream. Recent progress in detecting and tracking eddies[19,20] makes the quantification of the ring-driven flux timely. We identified all Gulf Stream cold-core rings in a database[19] of eddies detected in satellite altimetry data for 1993-2014 (Methods), and calculate that an average of 7.7±2.5 cyclonic rings cross the Gulf Stream each year (Suppl. Fig. 1), with an average surface area of $3.9\pm1.5\times10^4$ km^2 (the equivalent of a circular vortex, radius 111±70 km). As the ring identified at station USGT11-6 was shed many weeks before sampling (Methods) and its Fe inventory may thus have been affected by uptake, scavenging, or physical dissipiation of Fe, we chose not to use this ring as the endmember in our calculations. Instead, since cold-core rings enclose Slope Sea water pinched off by the Gulf Stream, we assumed that the average Fe concentration in Slope Water above the 1026.5 isopycnal (0.64±0.12 nmol kg^{-1}; stations USGT11-1 and 11-2) is representative of the initial dissolved Fe concentration in the core of the average cold core ring. We consider the water column above the 1026.5 isopycnal since we are interested in Fe that is accessible to NASG surface ecosystems over the annual cycle, and this isopycnal represents the density of the maximum NASG winter mixed layer.

If all rings dissipate entirely within the gyre, as assumed in an early study[29], their near-surface Fe burden would ultimately enter the subtropical mixed layer. In this view, the volume flux due to rings entering the gyre is balanced by an equivalent volume transport out of the gyre, largely due to warm-core rings, with the average Fe concentration of the interior gyre above the 1026.5 isopycnal (0.30±0.10 nmol kg^{-1}). Given the 0.34 nmol kg^{-1} Fe concentration difference and the ring statistics from satellite altimetry, the assumption of complete dissipation leads to a ring-driven Fe supply to the subtropical gyre of $0.3\pm0.17\text{x}10^{8}$ mol dissolved Fe yr^{-1}, accompanied by a dissolved phosphate supply of $1.8\pm1.1\text{x}10^{10}$ mol $year^{-1}$; Methods).

Our estimate of the ring-driven Fe and phosphate supply may be considered an upper limit, given that rings can be re-entrained into the Gulf Stream after only partial dissipation[30]. In these cases, only a fraction of the nutrients within the ring may be biologically consumed within the ring and/or mixed laterally with surrounding subtropical waters, before being re-entrained. A conservative estimate for the ring-driven nutrient supply is provided by assuming that nutrients become available only after physical dissipation of the rings, which assumes no biological consumption in the ring before re-entrainment. Assuming a lateral diffusivity of 300 m^2 s^{-1}, as diagnosed from float observations of analogous cold-core rings shed from the Kuroshio Extension[30], half of the volume-integrated Fe anomaly in the ring would be mixed with surrounding waters within two months, and ≤15% of the integrated Fe would remain at the end of one year (Methods; ED Fig. 2). With ring lifetimes thought to average more than a year[31], we estimate that accounting for re-entrainment of rings into the Gulf Stream after only partial dissipation would reduce our estimate by 15% at most. Additionally, rings are not the only processes that can transport Fe and nutrients across the Gulf Stream. Rather, a suite of mesoscale processes, including but not limited to rings, can mix nutrients down-gradient from the relatively high concentrations of the Slope Water into the NASG. We estimate that the total Fe supply due to down-gradient mixing across the Gulf Stream may be up to seven times larger than our ring-derived estimates (Methods).

Comparison of ring-derived fluxes with atmospheric supply. How does the ring-driven flux of soluble Fe to the NASG compare to that delivered by atmospheric deposition? Answering this question requires a robust quantification of atmospheric Fe fluxes, which are highly uncertain. Drawing upon a wide variety of independent observation- and model-based estimates, we have established a representative range of gyre-wide atmospheric Fe deposition fluxes to the NASG (Methods; Suppl. Info). A key uncertainty for the biogeochemical relevance of atmospheric Fe deposition is the solubility of the Fe delivered to the surface ocean. Different studies approach this question differently. For example, some models in our compilation include Fe as a prognostic variable and directly simulated its solubility; in these, Fe solubility in the dust deposited to the NASG ranged between ~1-2% (Table S1). In other studies, where only total Fe deposition was reported, we calculated soluble Fe delivery by assuming an appropriate upper bound of 5% solubility (see a more detailed discussion in Suppl. Info.). The resulting range of atmospheric soluble Fe fluxes over the entire subtropical gyre, an area of 8.75×10^{12} (see Suppl. Info.), spans a factor of more than 20, from 0.4-

8.6×10^8 mol Fe yr^{-1} (Fig. 4), with a median of 2×10^8 mol Fe yr^{-1}. Our estimate of ring-driven soluble Fe transport across one boundary of the NASG to the entire gyre thus represents between 3% and 75% of the range of estimated atmospheric deposition fluxes over the entire gyre surface, or 15% of the median deposition flux (Fig 4). In the face of the uncertainty of the magnitude of atmospheric soluble Fe supply, this result indicates that ring-driven transport of Fe across the Gulf Stream is quantitatively important for Fe supply to the gyre. When we consider that rings are unlikely to dissipate across the whole gyre, the importance of ring-driven transport becomes quantitatively more important in certain regions. Specifically, since the westward propagation of the rings means that they are most likely to dissipate within the north-western gyre, the ring-derived Fe flux may be considered as converging over just this region of the gyre. Fig. 4 shows how the ring-driven Fe flux per area varies as a function of the area over which the eddies are assumed to dissipate. This supply rate is compared to average gyre-wide dust fluxes. This scaling analysis suggests that if the rings dissipate within a band that is roughly 1000 km wide, along a 1000 km length of the Gulf Stream (that is an area of $1\text{x}10^6$ km^2), ring-driven transport of Fe may exceed the soluble Fe supply from dust in this region and thus could be the dominant mechanism of Fe supply to the western portion of the gyre (Fig. 4). Such a significant role for ocean circulation in Fe supply via lateral transport represents an important advance in understanding of sources of Fe to the subtropics, and parallels recognition of the importance of lateral transport for macronutrient budgets of subtropical gyres[15,18]. Our quantification of the ring-driven Fe flux suggests that such transport processes need to be included in Fe budgets and models of ocean biogeochemistry.

Implications for gyre biogeochemistry. Three other factors combine to reinforce the importance of cross-Gulf Stream Fe transport for the subtropical Fe budget and the biogeochemistry of the NASG. First, Slope Water contains a higher excess of Fe-binding ligands than the open surface gyre[32]. Not only does this mean that a higher percentage of the dissolved Fe coming from the Slope Sea may be bioavailable compared to dust-derived Fe, but a supply of excess ligands could also enhance *in situ* Fe dissolution from dust as well as stabilising the Fe thus released[33]. Second, organic matter C:P ratios are elevated above Redfield ratios within the gyre[34], suggesting there is higher productivity for each mole of phosphate transported into the gyre compared to outside. Thirdly, ring-driven Fe supply is known[14] to be accompanied by a supply of the macronutrients nitrate and phosphate to the gyre, and, importantly, an excess supply of phosphate relative to nitrate (Fig. 2d; Methods). In this study, our calculations yield a PO_4:NO_3 ratio of ring-driven transport of 1:11, i.e. an excess of PO_4 relative to the Redfield ratio of 1:16, consistent with previous results suggesting excess PO_4 supply to the NASG[14,35]. This observation is important, because creating a niche for diazotrophs relies on there being an excess of Fe and P over N[36].

In assessing whether ring-driven supply of nutrients and Fe could support diazotrophy in the NASG, resource-competition theory[37] suggests the supply of Fe and P relative to N across the Gulf Stream need to exceed their relative requirement by non-diazotrophic phytoplankton[31]. Therefore, the surplus PO_4 in rings should become available to diazotrophs following exhaustion of the NO_3 supply by non-diazotrophs. The corresponding Fe:NO_3 ratio in the rings is ~1:7500, or 0.13 mmol mol^{-1}. Cell quota studies[38] suggests that non-diazotrophic phytoplankton cells have Fe:N ratios of 0.06-0.31 mmol mol^{-1} N (reported Fe:PO_4 ratios of 1-5 mmol mol^{-1}, and converted assuming a Redfield N:P ratio). If the non-diazotrophic assemblage is comprised of cells at the low-end of this range, then the ring-driven nutrient supply could support diazotrophy. Otherwise, rings would be expected to leave surplus PO_4, but little Fe, behind after non-diazotrophic exhaustion of NO_3, priming the system for N_2 fixation in response to atmospheric Fe deposition events. Furthermore, we note that a similar dissolved Zn anomaly between slope Sea and Gyre was observed during GA03[39], meaning that rings also transport dissolved Zn into the gyre. If this dissolved Zn persists after utilisation of dissolved inorganic phosphate, it might be available to enhance alkaline phosphatase production and thus acquisition of phosphate from the dissolved phosphate pool[40,41], potentially by diazotrophs such as *Trichodesmium*[42,43].

We thus speculate that, dependent on the microbial and phytoplankton assemblage, and together with the stabilizing and solubilizing effect discussed above, ring-driven nutrient supply may contribute to the support of diazotrophy in the NASG, whilst also potentially influencing phosphate acquisition[12]. Even if ring transport of Fe does not support diazotrophy directly, ring transport of excess phosphate would still be expected to support diazotrophy in response to atmospheric Fe deposition events. More broadly, eddy-driven transport of Fe may be important in other similarly dynamic regions of the oceans, including the South Atlantic, where Agulhas rings carry elevated Fe concentrations into the subtropics[26], and the North Pacific, where Haida eddies carry Fe from Alaskan shelf waters to the Fe-limited open ocean[44]. Patchy supply of Fe and macronutrients by eddies may thus have a significant effect on local and regional biogeochemistry, playing an important and often-overlooked role in primary productivity, nitrogen fixation and carbon cycling within oligotrophic gyres.

References

1. Gruber, N. & Sarmiento, J. L. Global patterns of marine nitrogen fixation and denitrification. *Global Biogeochem. Cycles* **11,** 235–266 (1997).
2. Geider, R. J. & La Roche, J. The role of iron in phytoplankton photosynthesis, and the potential for iron-limitation of primary productivity in the sea. *Photosynth. Res.* **39,** 275–301 (1994).

3. Mahowald, N. M. *et al.* Atmospheric global dust cycle and iron inputs to the ocean. *Global Biogeochem. Cycles* **19,** GB4024 (2005).

4. Boyd, P. W. *et al.* Mesoscale iron enrichment experiments 1993-2005: synthesis and future directions. *Science* **315,** 612–7 (2007).

5. Moore, C. M. *et al.* Processes and patterns of oceanic nutrient limitation. *Nat. Geosci* **6,** 701–710 (2013).

6. Tagliabue, A. *et al.* The integral role of iron in ocean biogeochemistry. *Nature* **543,** 51–59 (2017).

7. Jickells, T. D., Baker, A. R. & Chance, R. Atmospheric transport of trace elements and nutrients to the oceans. *Philos. Trans. R. Soc. London A Math. Phys. Eng. Sci.* **374,** 20150286 (2016).

8. Moxim, W. J., Fan, S.-M. & Levy, H. The meteorological nature of variable soluble iron transport and deposition within the North Atlantic Ocean basin. *J. Geophys. Res.* **116,** D03203 (2011).

9. Sedwick, P. N. *et al.* Iron in the Sargasso Sea (Bermuda Atlantic Time-series Study region) during summer: Eolian imprint, spatiotemporal variability, and ecological implications. *Global Biogeochem. Cycles* **19,** (2005).

10. Conway, T. M. & John, S. G. Quantification of dissolved iron sources to the North Atlantic Ocean. *Nature* **511,** 212–215 (2014).

11. Moore, C. M. *et al.* Iron limits primary productivity during spring bloom development in the central North Atlantic. *Glob. Chang. Biol.* **12,** 626–634 (2006).

12. Browning, T. J. *et al.* Iron limitation of microbial phosphorus acquisition in the tropical North Atlantic. *Nat. Commun.* **8,** 15465 (2017).

13. Olson, D. B. Rings in the Ocean. *Ann. Rev. Earth. Planet. Sci.* **19**, 283-311 (1991).

14. Palter, J. B., Lozier, M. S., Sarmiento, J. L. & Williams, R. G. The supply of excess

phosphate across the Gulf Stream and the maintenance of subtropical nitrogen fixation. *Global Biogeochem. Cycles* **25,** GB4007 (2011).

15. Williams, R. & MJ, F. The Ekman transfer of nutrients and maintenance of new production over the North Atlantic. *Deep Sea Res. Pt I.* **45,** 461–489 (1998).

16. Williams, R. G. *et al.* Nutrient streams in the North Atlantic: Advective pathways of inorganic and dissolved organic nutrients. *Global Biogeochem. Cycles* **25,** GB4008 (2011).

17. Williams, R. G., Roussenov, V. & Follows, M. J. Nutrient streams and their induction into the mixed layer. *Global Biogeochem. Cycles* **20,** GB1016 (2006).

18. Letscher, R. T., Primeau, F. F. & Moore, J. K. Nutrient budgets in the subtropical ocean gyres dominated by lateral transport. **9,** 815–819 (2016).

19. Faghmous, J. H. *et al.* A daily global mesoscale ocean eddy dataset from satellite altimetry. *Sci. Data* **2,** 150028 (2015).

20. Mawji, E. *et al.* The GEOTRACES Intermediate Data Product 2014. *Mar. Chem.* **177,** 1–8 (2015).

21. Jenkins, W. J., Smethie, W. M., Boyle, E. A. & Cutter, G. A. Water mass analysis for the U.S. GEOTRACES (GA03) North Atlantic sections. *Deep Sea Res. Pt II.* **116,** 6–20 (2015).

22. Townsend, D. W. & Ellis, W. G. in *Nutrient Fluxes in Continental Margins: A Global Synthesis* (eds. Liu, K.-K., Atkinson, L., Quinones, R. & Alaue-McManus, L.) 7234–248 (Springer, 2010).

23. Palter, J. B., Lozier, M. S. & Barber, R. T. The effect of advection on the nutrient reservoir in the North Atlantic subtropical gyre. *Nature* **437,** 687–692 (2005).

24. Rijkenberg, M. J. A. *et al.* The distribution of dissolved iron in the West Atlantic Ocean. *PLoS One* **9,** e101323 (2014).

25. Middag, R. *et al.* Intercomparison of dissolved trace elements at the Bermuda Atlantic Time Series station. *Mar. Chem.* **177,** 476–489 (2015).

26. Conway, T. M., John, S. G. & Lacan, F. Intercomparison of dissolved iron isotope profiles from reoccupation of three GEOTRACES stations in the Atlantic Ocean. *Mar. Chem.* **183,** 50–61 (2016).

27. Wu, J. & Luther, G. W. Spatial and temporal distribution of iron in the surface water of the northwestern Atlantic Ocean. *Geochim. Cosmochim. Acta* **60,** 2729–2741 (1996).

28. Conway, T. M. & John, S. G. The cycling of iron, zinc and cadmium in the North East Pacific Ocean - Insights from stable isotopes. *Geochim. Cosmochim. Acta* **164,** 262-283 (2015).

29. Bower, A. S., Rossby, H. T. & Lillibridge, J. L. The Gulf Stream: Barrier or blender? *J. Phys. Ocean.* **15,** 24–32 (1985).

30. Qiu, B., Chen, S. & Hacker, P. Effect of mesoscale eddies on subtropical mode water variability from the Kuroshio Extension System Study (KESS). *J. Phys. Oceanogr*. **37,** 982–1000 (2007).

31. Lai, D. Y., Richardson, P. L., Lai, D. Y. & Richardson, P. L. Distribution and Movement of Gulf Stream Rings. *J. Phys. Oceanogr.* **7,** 670–683 (1977).

32. Buck, K., Sohst, B. M. & Sedwick, P. N. The organic complexation of dissolved iron along the U.S. GEOTRACES (GA03) North Atlantic Section. *Deep Sea Res. Pt II.* **116,** 152–165 (2015).

33. Fishwick, M. P. *et al.* The impact of changing surface ocean conditions on the dissolution of aerosol iron. *Global Biogeochem. Cycles* **28,** 1235–1250 (2014).

34. Moreno, A. R. & Martiny, A. C. Ecological Stoichiometry of Ocean Plankton. *Ann. Rev. Mar. Sci.* **10,** 43–69 (2018).

35. Deutsch, C., Sarmiento, J. L., Sigman, D. M., Gruber, N. & Dunne, J. P. Spatial coupling of nitrogen inputs and losses in the ocean. *Nature* **445,** 163–167 (2007).

36. Ward, B. A., Dutkiewicz, S., Moore, C. M. & Follows, M. J. Iron, phosphorus, and nitrogen supply ratios define the biogeography of nitrogen fixation. *Limnol. Oceanogr.* **58,** 2059–2075 (2013).

37. Tilman, D. Resource Competition between Plankton Algae: An Experimental and Theoretical Approach. *Ecology* **58,** 338–348 (1977).

38. Twining, B. S. & Baines, S. B. The trace metal composition of marine phytoplankton. *Ann. Rev. Mar. Sci.* **5,** 191–215 (2013).

39. Conway, T. M. & John, S. G. The biogeochemical cycling of zinc and zinc isotopes in the North Atlantic Ocean. *Global Biogeochem. Cycles* **28,** 1111-1128 (2014).

40. Shaked, Y., Xu, Y., Leblanc, K. & Morel, F. M. M. Zinc availability and alkaline phosphatase activity in Emiliania huxleyi: Implications for Zn-P co-limitation in the ocean. *Limnol. Oceanogr.* **51,** 299–309 (2006).

41. Mahaffey, C., Reynolds, S., Davis, C. E. & Lohan, M. C. Alkaline phosphatase activity in the subtropical ocean: insights from nutrient, dust and trace metal addition experiments. *Front. Mar. Sci.* **1,** 73 (2014).

42. Orcutt, K., Gundersen, K. & Ammerman, J. Intense ectoenzyme activities associated with Trichodesmium colonies in the Sargasso Sea. *Mar. Ecol. Prog. Ser.* **478,** 101–113 (2013).

43. Sohm, J. A., Mahaffey, C. & Capone, D. G. Assessment of relative phosphorus limitation of Trichodesmium spp. in the North Pacific, North Atlantic, and the north coast of Australia. *Limnol. Oceanogr.* **53,** 2495–2502 (2008).

44. Xiu, P., Palacz, A. P., Chai, F., Roy, E. G. & Wells, M. L. Iron flux induced by Haida eddies in the Gulf of Alaska. *Geophys. Res. Lett.* **38,** L13607 (2011).

Acknowledgements

We thank all those who contributed to the US GEOTRACES GA03 cruises; the GEOTRACES Program and the Ocean Data Facility who supplied the supporting physical parameters for the USGT11 cruise; Natalie Mahowald, Samuel Albani, Akinori Ito and Rong Wang for making model output available; and Peter Sedwick, Bill Landing, Natalie Mahowald, Chris Measures and Derek Vance for useful discussions. TMC acknowledges support from the University of South Florida; JBP acknowledges support from the University of Rhode Island; GFdS is supported by the European Union's Horizon 2020 research and innovation programme under Marie Skłodowska-Curie grant agreement #708407.

Author Contributions

All authors contributed equally to this work, TMC and GFdS conceived the idea, JBP carried out the ring-driven Fe transport calculations and GFdS carried out the atmospheric deposition calculations.

Additional Information

Supplementary Information is available in the online version of the paper. Reprints and permissions information is available online at www.nature.com/reprints. Correspondence and requests for materials should be addressed to TMC.

Competing Financial Interests

The authors declare no competing financial interests.

Figure Captions

Figure 1. GA03 Fe station sampling locations[20], Gulf Stream and cold-core ring in satellite altimetry. Satellite observations of sea-surface height (metres, black contours at 0.52 and 0.55 m) from the AVISO merged mean absolute dynamic topography product (November 9th–16th 2011) show that Station 6, sampled along the GEOTRACES GA03 (USGT11) section (black line) on November 14, 2011, was at the edge of a cold-core ring. Weekly AVISO data shows that the ring was shed from the Gulf Stream between September 28 and October 8, 2011 (see Suppl. Animation 2).

Figure 2. A cold-core ring observed in the GA03 section. The transition from (a) poorly-oxygenated, fresh, Fe- and P-rich waters of the Slope Sea in the west to well-oxygenated, salty, Fe- and P-depleted waters of the gyre[10,21]. Stations are numbered, and sampling depths marked by dots. To the east of the Gulf Stream (centred around Station 3), the upward doming of isopycnals mark the cold-core ring (Station 6). Two additional stations within the Gulf Stream improve the spatial resolution of oxygen, salinity and phosphate data, which resolve the transition between the gyre and the ring more clearly than the Fe distribution.

Figure 3. GA03 Temperature-salinity diagram, with Fe concentrations[10] in colour. The Slope Sea (grey) has low temperature, low salinity and elevated Fe near the σ_θ = 26.5 isopycnal (dashed grey) relative to the NASG (pink). The dashed black line represents Station 6 at the edge of the ring, with temperature-salinity showing strong interleaving between the Slope Sea and NASG. Ring Fe concentrations are also elevated, especially relative to Fe-depleted STMW around the σ_θ = 26.5 isopycnal that dominates the subsurface NASG (Fig. 2). Grey contours show potential density anomaly σ_θ in units of kg m^{-3}.

Figure 4. Ring-driven dissolved Fe supply compared to atmospheric dissolved Fe deposition. Based on our estimate of total ring-driven Fe supply to the NASG, we calculate the supply per unit area as a function of the area over which the ring-driven supply converges (red line; shading denotes uncertainty), ranging from a small region very near the Gulf Stream to the entire gyre. Horizontal lines show atmospheric deposition of soluble Fe to the entire NASG from modelling and observational studies. Black lines represent studies that modelled Fe solubility explicitly, while blue lines represent those to which we applied 5% Fe solubility (Suppl. Info.).

Methods

Data availability. GA03 dissolved Fe concentration data shown in Figs. 2-3 and used in calculations are taken from Conway and John[10]. Supporting data for macronutrients, salinity and temperature along GA03 are reproduced from the Ocean Data Facility[21] and all GA03 data are freely available[20] in the GEOTRACES Intermediate Data Product 2014 and 2017. The satellite data used in this work to calculate eddy size and number from Faghmous *et al.*[19] is freely available from https://datadryad.org//resource/doi:10.5061/dryad.gp40h.

***Satellite-derived eddy database*.** Faghmous *et al.*[19] provide a database of eddies detected in satellite altimetry, compiled for the years 1993-2014. In this database, a cyclonic eddy is defined as the outermost closed contour of altimetric sea level anomaly (SLA) containing a single minimum in sea level. This minimum is defined as a grid cell whose SLA is less than its surrounding 24 neighbouring grid points (on a 5×5 grid), where each side of a grid box is 0.25° in latitude or longitude. To track the eddies over time, all eddies in the next day SLA image within a geographical boundary are checked to see whether there is an eddy that qualifies to be stitched to the current day's eddy to form a track. This geographical boundary accounts for westward propagation at the Rossby phase speed.

Cross-Gulf Stream ring identification. Using the Faghmous *et al.*[19] database, we identified and recorded the size of cold-core rings that cross the climatological Gulf Stream position into the subtropical gyre as follows: 1) Construct a monthly climatology of sea surface height (SSH) over the satellite record; 2) Interpolate the monthly mean climatological SSH along each cyclonic eddy track in the vicinity of the Gulf Stream; 3) Tag any eddies that cross from north of the climatological Gulf Stream position (regions with SSH below 0.52 m from the AVISO absolute dynamic topography) to the subtropical side of the Gulf Stream (SSH greater than 0.55 m) and persist as a coherent track for at least three weeks.

We compared the performance of this objective identification against an ad-hoc visual assessment for a random subset of the satellite record (comprising 8 years and 66 eddies – more than a third of all cold-core rings from the final record). For two examples of this ad-hoc visual assessment, see Suppl. Animation 1 for a clear example of a cold core ring penetrating into the subtropical gyre from 1993, and Suppl. Animation 2 for the ring sampled at station USGT11-6 from 2011. The eddies identified by the algorithm generally have the expected characteristics of a cold-core ring: they are formed from a steep meander of the Gulf Stream, shed to the south, and propagate westward. Moreover, the eddy amplitude (i.e. the absolute value of the sea level anomaly along the track) is 46 cm, further verifying that these rings travel across the position of the climatological Gulf Stream and are, thus, large negative anomalies relative to the average subtropical sea-surface height. Furthermore, our estimate of ring number, 7.7 ± 2.5 rings yr^{-1} (Suppl. Fig. 1), is within the uncertainty bounds of earlier work that counted the number of rings identified by cold anomalies in satellite sea surface temperature snapshots and divided by an estimate of their lifetime[45].

Estimation of dissolved Fe anomaly in a ring. We estimated the dissolved Fe concentration within a cold-core ring based on the Slope Sea stations from the GA03 Section dataset[10]. To do this, we calculated the depth integrated average Fe concentration observed in near-surface layers (i.e. in and above the density of the STMW, isopycnal 1026.5). The 1026.5 isopycnal was at depths of ~100 m in the Slope Sea, deepening to 350 m in the open gyre (Fig. 2), and is taken as the deepest relevant depth of Fe that may become available for productivity in the gyre, since this isopycnal represents the maximum winter mixed layer density in the gyre[46]. Taking data from 0-100 m at stations USGT11-1 and -2 within the Slope Sea gave an average of 0.64 nmol kg^{-1} for the Slope Sea, with a standard deviation of 0.12 nmol kg^{-1}. Similarly, taking the mean of data from 0 to 350 m at GA03 stations USGT11-8 and USGT11-10, to represent the interior of the gyre, gave 0.30 nmol kg^{-1}, with a standard deviation of 0.10 nmol kg^{-1}. We excluded the outlier top data point at Station 8 (1.2 nmol kg^{-1}) from the average to preclude any effect from recent dust deposition or contamination biasing the gyre average. The calculated Fe anomaly (ΔFe) within an average cold-core ring is thus assumed to be the difference between these numbers (0.34 nmol kg^{-1}). We chose not to use the average observed ring concentrations from above the 1026.5 isopycnal or above 500 m at USGT11-6 (0.37 and 0.47 nmol kg^{-1} respectively) as the Slope Water end member, because it is clear from SSH data that (a) station USGT11-6 was at the edge of the ring and (b) the ring was shed about 5–6 weeks before sampling, and thus has presumably lost significant Fe due to scavenging, biological uptake, and mixing with subtropical waters, as suggested by the strong interleaving seen in Fig. 3 (Fe dissipation estimate below).

Calculation of ring-driven Fe transport. We calculated the total ring-driven supply of Fe to the NASG (φ_{Fe}) as the product of the Fe anomaly in a ring relative to subtropical concentrations (ΔFe) times the number of rings (*n*), their surface area (*A*), and a characteristic depth scale of the Fe anomaly accessible to the surface ocean over a seasonal cycle (*D*):

$$\varphi_{Fe} = \Delta\text{Fe} \times n \times A \times D \qquad (1)$$

where ΔFe = 0.34 µmol m^{-3} (equivalent to 0.34 nmol kg^{-1}), n = 7.7 rings yr^{-1}, $A = 3.9\times10^4$ km^2, and D = 300, which is the depth of a typical mixed layer in the subtropical mode water formation region[46]. Under these assumptions, the total ring-driven supply of Fe is equal to $0.3\pm0.17\times10^8$ mol dissolved Fe $year^{-1}$. The uncertainty is propagated from the standard deviations of the ring number (7.7±2.5 per year), size ($3.9\pm1.5\times10^4$ km^2), and Fe concentrations (0.2 µmol m^{-3}), and includes an estimate of uncertainty on *D* of 50 m. This calculation makes the implicit assumption that the volume transport by cold core rings into the subtropical gyre (represented by $n \times A \times D$) is balanced by an equal volume transport out of the subtropical gyre with Fe concentrations equal to those observed in the GA03 subtropical stations.

Estimation of the Fe dissipation from the ring. To estimate the amount of Fe that would dissipate from a cold-core ring during its time in the gyre, we use the same diffusivity as was observed for cold-core rings shed from the Kuroshio Extension[30]. We assume a circular vortex[30] with initial tracer concentration:

$$\text{Fe}(r,0) = \text{Fe}_o + \text{Fe}_1 exp(\frac{-r^2}{a^2}) \qquad (2)$$

where Fe_o is the subtropical Fe concentration, taken to be 0.30 µmol m^{-3}; (equivalent to 0.30 nmol kg^{-1}); Fe_1 is the Fe anomaly at the centre of the ring relative to the background concentration, set at 0.34 µmol m^{-3} (equivalent to 0.34 nmol kg^{-1}); r is the distance from the ring's centre; and a^2 sets the exponential decay length scale, taken to be 48 km, as was found to be appropriate for a ring of about 100 km radius by Qiu and colleagues[30]. The isopycnal diffusion of Fe out of the ring proceeds according to:

$$\frac{\partial \mathrm{Fe}(r,t)}{\partial t} = A_h \frac{1}{r}\frac{\partial}{\partial r}\left[r\frac{\partial \mathrm{Fe}(r,t)}{\partial r}\right] \quad (3)$$

where A_h is the diffusivity, taken to be equal to 300 m^2 s^{-1} as found for the cold-core rings shed from the Kuroshio[30]. Suppl. Fig. 2a. shows the solution to this equation at various times, and illustrates the rapid loss of Fe from the ring core. Suppl. Fig. 2b quantifies the integrated Fe anomaly in the central 50 km of the ring (relative to the background subtropical concentration) as a function of time. These results show that after only 2 months, the ring would lose half of its integrated Fe anomaly, with less than 15% remaining after 1 year. These timescale calculations are consistent with the observation of strong interleaving within the ring in the GA03 section (Fig. 3), which satellite data suggest was shed from the Gulf Stream 5–6 weeks before it was sampled.

Comparison of ring-driven flux to scaling for total down-gradient mixing of Fe and other terms in the Fe conservation equation. A basic scale analysis of the down-gradient transport of Fe provides a check on the order of magnitude of the ring-based estimate. Such along-isopycnal diffusion scales as $\frac{A_h D \Delta \mathrm{Fe}}{L^2}$, where A_h is the isopycnal diffusivity, with estimates of A_h ranging from 500 to 1500 m^2 s^{-1}; D is the thickness of the vertical layer of interest (nominally the 300 m depth of a typical winter mixed layer just south of the Gulf stream[46]); ΔFe is the difference in Fe concentrations across the Gulf Stream of 0.34 nmol kg^1; and L is the horizontal length scale over which the Fe change is observed (i.e. about 50 km). We note that these diffusivity estimates for A_h may be higher than that used to estimate the mixing out of the rings above, as turbulent diffusivity scales with the length over which the turbulent motions are averaged[47]. With these parameter choices, the down-gradient diffusion of Fe into the subtropical gyre is estimated as supplying 480-1450 μmol m^{-2} $year^{-1}$, with the range coming from the range of A_h values (500 to 1500 m^2 s^{-1}). For a Gulf Stream length along the Slope Sea of 2000 km and over a 50 km width, the total supply of Fe due to down-gradient diffusion is estimated at between 0.3×10^8 and 2×10^8 mol year^{-1}. This calculation yields a flux that is up to 7 times larger than the ring-derived estimate. We take the agreement in order of magnitude between the low end of this estimate with that derived from the ring statistics as an indication that the ring-based estimate of Fe supply is within reasonable limits. That the diffusion-based estimate may be substantially larger than the ring-based estimate is consistent with the idea that rings are one of many mesoscale processes moving Fe from the Slope Sea across the Gulf Stream.

This isopycnal mixing term is one of several physical mechanisms that can potentially transport Fe into or out of the subtropical gyre, in the layer above the annual maximum mixed layer. Following the approach in Williams and Follows[15], we provide a scale analysis of the following additional transport terms for comparison to the ring-driven transport. On a seasonal basis, the vertical entrainment term may dominate phosphate and nitrate budgets[15], since there is an accumulation of these macronutrients in the seasonal pycnocline. However, iron is depleted to depths below even the permanent pycnoocline (i.e. below the 26.5 isopycnal). Thus, we expect vertical entrainment to be a small term, and may cause dilution of the iron deposited on the ocean surface through a deepening mixed layer. In any case, for an iron budget integrated to the base of the deepest annual mixed layer, the vertical entrainment term is approximately offset by the biological export term[15], and we expect the budget to be dominated by Ekman advection, diapycnal mixing, and vertical advection, each of which is scaled in the following analysis.

Ekman advection is estimated from the average down-front winds along the Gulf Stream, which create Ekman transports of $U = 2$ m^2 s^{-1} (equivalent to 4 cm s^{-1} over an Ekman layer of 50 m depth[14]) acting across surface Fe concentrations that decrease from 0.6 to 0.3 µmol m^{-3} going southward across the Gulf Stream. Therefore, over a length scale of order 50 km, we estimate an Ekman transport convergence, $\frac{\Delta UFe}{\Delta y}$, of O(10^{-4}) μmol m^{-2} year^{-1}. This is many orders of magnitude smaller than that due to ring-driven transport (Fig. 4), even assuming convergence over a broad area. The dominance of eddies in the lateral transport term agrees with the results from a recently-submitted manuscript based on the results of a 1/10° ocean model (Yamamoto A. *et al*., unpublished data). Diapycnal mixing at the base of the maximum wintertime mixed layer appears to be an extraordinarily small term, since there is a homogenous, low-Fe layer extending all the way to the 1026.75 isopycnal, well beneath the densest subtropical mixed layer (<1026.5). This term scales as $A_v \frac{\Delta Fe}{D}$, where A_v is a turbulent diapycnal diffusivity, typically O(10^{-5}), and ΔFe is the vertical iron difference over some depth, *D,* at the base of the annual maximum mixed layer. Since the vertical Fe gradient is essentially zero near the base of this layer, so too will the turbulent mixing supply be close to zero. Finally, vertical advection is also a small Fe removal term at the base of the annual maximum mixed layer, given the slow downwelling velocities, O(25 m year^{-1}), acting on the low Fe concentrations 0.3 umol m^3 to yield an estimate for this term of $w\mathrm{Fe}|_{z=D}$ of -7 μmol m^2 year^{-1}. Hence, the mesoscale eddy-driven supply of Fe and atmospheric deposition appear to far exceed any other physical transport mechanisms. In steady state, the sum of Fe export in biogenic and other sinking particles should balance these supply terms.

Calculation of cross-Gulf Stream phosphate and nitrate fluxes. Analogous calculations to those for Fe can be made for the ring-driven supply of dissolved phosphate and nitrate, with these calculations advantaged by much greater data coverage. Using GA03 dissolved nutrient data, as well as 7 much higher-resolution sections across the Gulf Stream (6 from the CLIMODE program in January 2006 and February/March 2007[14,48], and 1 from cruise EN596 in April 2017 (J. B. Palter, unpublished data), we find that phosphate concentrations just north of the Gulf Stream and above the 1026.5 isopycnal are, on average, 0.2 mmol m^{-3}

higher than for the same layer on the subtropical side of the Gulf Stream, whilst for nitrate the corresponding difference is 2.25 mmol m^{-3}. Given the ring characteristics from the altimetry detection and tracking as above, we estimate a ring-driven phosphate supply of $1.8\times10^{10}\pm1.1\times10^{10}$ mol $year^{-1}$ and a nitrate supply of $20\times10^{10}\pm 2\times10^{10}$ mol $year^{-1}$, with uncertainties based on ring statistics as for Fe, and also including variability in phosphate and nitrate concentrations. For comparison, a study using a data-constrained ocean model[18] estimated a lateral supply of phosphate plus dissolved organic phosphorus to the North Atlantic subtropical gyre of approximately 3.2×10^{10} mol P year, most of which occurs on the southern fringe of the Gulf Stream. In that coarse-resolution model study, the supply due to lateral mean flow and parameterized eddy mixing was combined into one term that was approximately a factor of 2.5 greater than our estimate for the rings alone, corroborating that rings are likely to provide an important fraction of the total cross-Gulf Stream nutrient supply.

Calculation of atmospheric Fe deposition fluxes to the subtropical gyre. Accurate estimation of soluble Fe flux to the oceans requires knowledge of three parameters: a) aerosol deposition flux; b) Fe content of the deposited aerosols; and c) the fraction of deposited Fe that dissolves in seawater. Whilst the Fe content of mineral aerosol, and Saharan dust in particular, has been shown to be very similar to that of average upper continental crust[49–52], uncertainties on the other two parameters are large, even leading to disagreement by several orders of magnitude on dust deposition fluxes to the same region[53]. We represent this range in uncertainty by estimating soluble Fe deposition to the NASG using a wide variety of methods, including both extrapolation from observational estimates in the eastern Atlantic close to the Saharan source[54–56] and at Bermuda in the western Atlantic[57], as well as integration of simulated atmospheric deposition fluxes from numerous modelling studies[3,58–

[63] (Suppl. Info.). The fractional solubility of Fe in atmospheric aerosols ranges from <1% to >95% with a median value of ~3% in the Atlantic Ocean[57]. Data compilations as well as studies within the subtropical North Atlantic near Bermuda show that remote marine aerosols have fractional Fe solubility higher than the values of <1% observed for fresh mineral dust, perhaps the result of source composition, natural physical or chemical processing during atmospheric transport, or the increased importance of aerosols from anthropogenic combustion sources[7,33,57,64,65]. We choose an upper-bound estimate for the solubility of Fe in atmospheric aerosols deposited in the subtropical North Atlantic of 5%, which is among the highest seen in the literature for this region (Suppl. Info.). Thus, our estimate of ring-mediated transport of Fe is compared to what is likely to be a maximum estimate of the atmospheric source. See Suppl. Info. for an extended discussion of all the models and details of the calculations carried out to generate the range described in the main text.

Additional Method References

45. Richardson, P. L., Cheney, R. E. & Worthington, L. V. A census of Gulf Stream rings, spring 1975. *J. Geophys. Res.* **83,** 6136 (1978).

46. de Boyer Montégut, C., Madec, G., Fischer, A. S., Lazar, A. & Iudicone, D. Mixed layer depth over the global ocean: An examination of profile data and a profile-based climatology. *J. Geophys. Res.* **109,** C12003 (2004).

47. LaCasce, J. H. Statistics from Lagrangian observations. *Prog. Oceanogr.* **77,** 1–29 (2008).

48. The Climode Group. The Climode Field Campaign: Observing the Cycle of Convection and Restratification over the Gulf Stream. *Bull. Am. Meteorol. Soc.* **90,** 1337–1350 (2009).

49. Trapp, J. M., Millero, F. J. & Prospero, J. M. Trends in the solubility of iron in dust-dominated aerosols in the equatorial Atlantic trade winds: Importance of iron speciation and sources. *Geochemistry, Geophys. Geosystems* **11,** Q03014 (2010).

50. Shelley, R. U., Morton, P. & Landing, W. M. Elemental ratios and enrichment factors in aerosols from the US-GEOTRACES North Atlantic transects. *Deep Sea Res. Pt II.* **116,** 262–272 (2015).

51. Patey, M. D., Achterberg, E. P., Rijkenberg, M. J. & Pearce, R. Aerosol time-series measurements over the tropical Northeast Atlantic Ocean: Dust sources, elemental composition and mineralogy. *Mar. Chem.* **174,** 103–119 (2015).

52. Taylor, S. R. & McLennan, S. M. The continental crust: Its composition and evolution. Blackwell Scientific Publishing (1985).

53. Anderson, R. F. *et al.* How well can we quantify dust deposition to the ocean? *Philos. Trans. R. Soc. London A Math. Phys. Eng. Sci.* **374,** 20150285 (2016).

54. Measures, C. I., Hatta, M., Fitzsimmons, J. N. & Morton, P. Dissolved Al in the zonal N Atlantic section of the US GEOTRACES 2010/2011 cruises and the importance of hydrothermal inputs. *Deep Sea Res. Pt II.* **116,** 176–186 (2015).

55. Baker, A. R., Adams, C., Bell, T. G., Jickells, T. D. & Ganzeveld, L. Estimation of atmospheric nutrient inputs to the Atlantic Ocean from 50°N to 50°S based on large-scale field sampling: Iron and other dust-associated elements. *Global Biogeochem. Cycles* **27,** 755–767 (2013).

56. Powell, C. F. *et al.* Estimation of the Atmospheric Flux of Nutrients and Trace Metals to the Eastern Tropical North Atlantic Ocean. *J. Atmos. Sci.* **72,** 4029–4045 (2015).

57. Sholkovitz, E. R., Sedwick, P. N., Church, T. M., Baker, A. R. & Powell, C. F. Fractional solubility of aerosol iron: Synthesis of a global-scale data set. *Geochim. Cosmochim. Acta* **89,** 173–189 (2012).

58. Luo, C. *et al.* Combustion iron distribution and deposition. *Global Biogeochem. Cycles* **22,** GB1012 (2008).

59. Albani, S. *et al.* Paleodust variability since the Last Glacial Maximum and implications for iron inputs to the ocean. *Geophys. Res. Lett.* **43,** 3944–3954 (2016).

60. Albani, S. *et al.* Improved dust representation in the Community Atmosphere Model. *J. Adv. Model. Earth Syst.* **6,** 541–570 (2014).

61. Zhang, Y. *et al.* Modeling the global emission, transport and deposition of trace elements associated with mineral dust. *Biogeosciences Discuss.* **11,** 17491–17541 (2015).

62. Wang, R. *et al.* Sources, transport and deposition of iron in the global atmosphere. *Atmos. Chem. Phys.* **15,** 6247–6270 (2015).

63. Ito, A. & Shi, Z. Delivery of anthropogenic bioavailable iron from mineral dust and combustion aerosols to the ocean. *Atmos. Chem. Phys.* **16,** 85–99 (2016).

64. Conway, T. M., Wolff, E. W., Röthlisberger, R., Mulvaney, R. & Elderfield, H. E. Constraints on soluble aerosol iron flux to the Southern Ocean at the Last Glacial Maximum. *Nat. Commun.* **6,** 7850 (2015).

65. Longo, A. F. *et al.* Influence of Atmospheric Processes on the Solubility and Composition of Iron in Saharan Dust. *Environ. Sci. Technol.* **50,** 6912–6920 (2016).

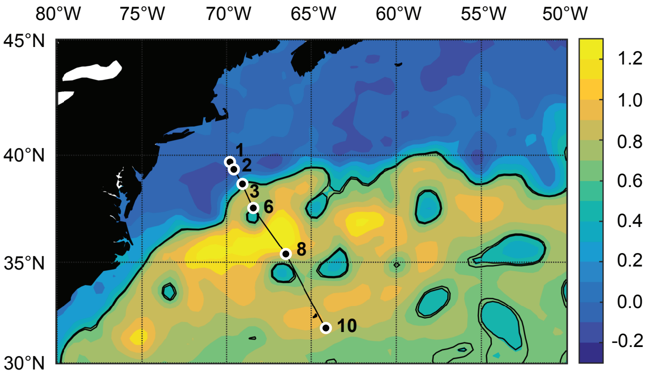

80°W
75°W
70°W
65°W
60°W
55°W
50°W
45°N
40°N
35°N
30°N
1
2
3
6
8
10
1.2
1.0
0.8
0.6
0.4
0.2
0.0
-0.2

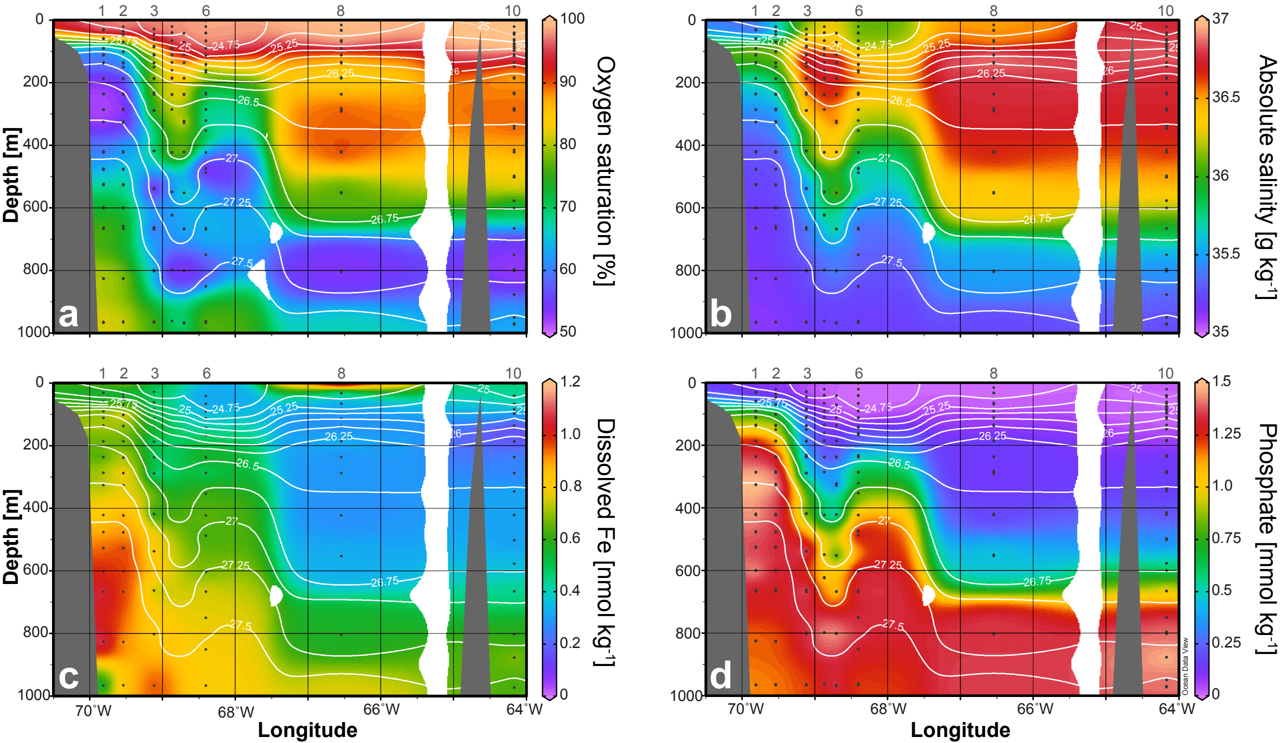
a
b
c
d
Depth [m]
Longitude
Oxygen saturation [%]
Absolute salinity [g kg-1]
Dissolved Fe [nmol kg-1]
Phosphate [mmol kg-1]
70°W
68°W
66°W
64°W
1
2
3
6
8
10
Ocean Data View

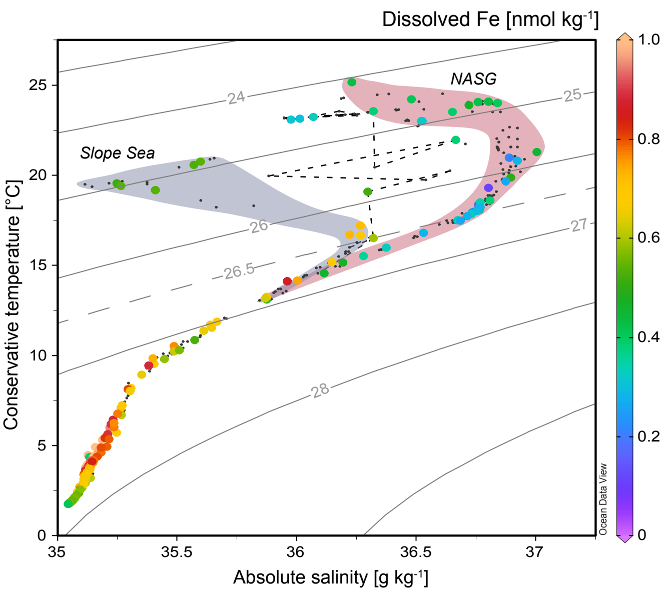

Dissolved Fe [nmol kg⁻¹]
1.0
0.8
0.6
0.4
0.2
0
NASG
Slope Sea
24
25
26
26.5
27
28
Conservative temperature [°C]
25
20
15
10
5
0
Absolute salinity [g kg⁻¹]
35
35.5
36
36.5
37
Ocean Data View

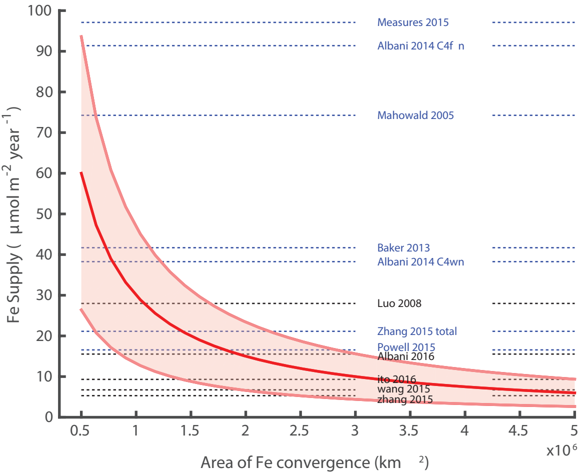

Measures 2015
Albani 2014 C4f n
Mahowald 2005
Baker 2013
Albani 2014 C4wn
Luo 2008
Zhang 2015 total
Powell 2015
Albani 2016
ito 2016
wang 2015
zhang 2015
Fe Supply (μmol m⁻² year⁻¹)
Area of Fe convergence (km²)
x10⁶
0
10
20
30
40
50
60
70
80
90
100
0.5
1
1.5
2
2.5
3
3.5
4
4.5
5